Available online at www.sciencedirect.com
ScienceDirect
Journal of Solid State Chemistry 179 (2006) 3695–3703
JOURNAL OF SOLID STATE CHEMISTRY
www.elsevier.com/locate/jssc

# Heterobimetallic thiocyanato-bridged coordination polymers based on $[Hg(SCN)_4]^{2-}$: Synthesis, crystal structure, magnetic properties and ESR studies

Fang-Fang Jian*, Hai-Lian Xiao, Fa Qian Liu

*New Materials & Function Coordination Chemistry Laboratory, Qingdao University of Science and Technology, Qingdao Shandong 266042, PR China*

Received 13 March 2006; received in revised form 22 July 2006; accepted 7 August 2006
Available online 9 August 2006

**Abstract**

Three new M/Hg bimetallic thiocyanato-bridged coordination polymers; $[Hg(SCN)_4Ni(Im)_3]_\infty$ **1**, $[Hg(SCN)_4Mn(Im)_2]_\infty$ **2**, and $[Hg(SCN)_4Cu(Me\text{-}Im)_2\ Hg(SCN)_4Cu(Me\text{-}Im)_4]_\infty$ **3**, (Im = imidazole, Me-Im = *N*-methyl-imidazole), have been synthesized and characterized by means of elemental analysis, ESR, and single-crystal X-ray. X-ray diffraction analysis reveals that these three complexes all form 3D network structure, and their structures all contain a thiocyanato-bridged Hg···M···Hg chain (*M* = Mn, Ni, Cu) in which the metal and mercury centers exhibit different coordination environments. In complex **1,** the $[Hg(SCN)_4]^{2-}$ anion connects three $[Ni(Im)_3]^{2+}$ using three SCN ligands giving rise to a 3D structure, and in complex **2,** four SCN ligands bridge $[Hg(SCN)_4]^{2-}$ and $[Mn(Im)_2]^{2+}$ to form a 3D structure. The structure of **3** contains two copper atoms with distinct coordination environment; one is coordinated by four *N*-methyl-imidazole ligands and two axially elongated SCN groups, and another by four SCN groups (two elongated) and two *N*-methyl-imidazole ligands. The magnetic property of complex **1** has been investigated. The spin state structure in hetermetallic NiHgNi systems of complex **1** is irregular. The ESR spectra results of complex **3** demonstrate $Cu^{2+}$ ion lie on octahedral environment.


*Keywords:* Coordination polymer; Heterometallic complexes; $Hg(SCN)_4^{2+}$; Magnetic properties

## 1. Introduction

Coordination polymers are one of the most interesting topics in current chemistry and crystal engineering. One of the possible strategies to improve the selectivity toward the reactivity of coordination polymers is to synthesize inorganic–organic hybrid frameworks with different metal coordination environments, as has been observed in some metalloenzymes [1]. To choose an appropriate starting building block for such design, the synthesis has been identified as a useful tool in the construction of inorganic–organic hybrid frameworks. Recently, the strategy of using metal complex cations and various pseudohalide or pseudochalcogenide or organic carboxylates as starting building blocks to give extended networks has been of great interest for the chemist [2–5]. This synthetic strategy offers prospect of rationally designing extended solids with desired properties by linking together molecular building blocks with specific functionality and geometry.

Thiocyanate is an ambidentate ligand capable of bridging two metal centers in an asymmetric mode through N-end attached to one metal and S-end to another one. In general, the choice of the thiocyanometallate is limited, since the geometry of the complexes are restricted to, e.g. linear as in $[Ag(SCN)_2]^-$, tetrahedral as in $[Cd(SCN)_4]^{2-}$ and $[Hg(SCN)_4]^{2-}$, square planar as in $[Ni(SCN)_4]^{2-}$ and $[Pd(SCN)_4]^{2-}$, and octahedral $[M(SCN)_6]^{3-}$ [6,7]. The second coordination center, however, can be almost any metal ion in the Periodic Table. Usually, the transition metal ion is selected because of the existence of a $\sigma$–$\pi$ feedback bond between the selected metal ion and the thiocyano group which enables production of more stable complexes. Our group selected group IIB metal thiocyano

*Corresponding author. Fax: +86 532 84023606.
*E-mail address:* ffj2003@163169.net (F.-F. Jian).

0022-4596/$ - see front matter © 2006 Elsevier Inc. All rights reserved.
doi:10.1016/j.jssc.2006.08.001

complexes, capable of $d^{10}$ metal atom, such as $[Hg(SCN)_4]^{2-}$ anion, as building unit to bridge some metal complex cations $[M(L)_n]^{2+}$ ($M = Mn^{2+}$, $Fe^{2+}$, $Co^{2+}$, $Ni^{2+}$, $Cu^{2+}$; $L$ = neutral ligands) to build a multidimensional structure. We have tried to elucidate how the structure of metal complexes anions can act as an effective tool in controlling the structure. However, it is difficult to get the single crystal structure of these bimetallic coordination polymers because these polymers are often low solubility in common organic solvents. One way to circumvent this practical problem is to introduce bulky organic ligands into the polymers to increase their solubility. Imidazole and *N*-methyl-imidazole was selected for this purpose. Imidazole is of considerable interest as a ligand in many biological systems in which it provides a potential binding site for metal ions [8]. Imidazole itself is an unidentate ligand and forms complexes with metal ions through its tertiary nitrogen atoms. Some complexes of imidazole and its derivatives with transition metal ions have been reported by our group [9]. In this paper, we report the synthesis, single crystal structures of three new heterobimetallic thiocyanato-bridged Hg–Ni, Hg–Mn and Hg–Cu coordination polymers. Also, the magnetic property of complex **1,** and the ESR spectra results of complex **1** and **3** have been investigated.

## 2. Experimental section

### 2.1. Measurements

Elemental analyses for carbon, hydrogen and nitrogen were performed using a Perkin-Elmer 240C elemental instrument. Variable-temperature magnetic susceptibilities were measured on a Quantum Design MPMS-7 SQUID magnetometer. The powder ESR spectra were recorded on a Bruker 2000-SRC spectrometer. Thermal gravity (TG) and differential analysis (DTA) were recorded on a SDT 2980 simultaneously for the samples of ca. 10 mg under a nitrogen atmosphere (150 ml/min) at a heating rate of 10 °C/min.

### 2.2. Synthesis

All chemicals were of analytical reagent grade and used directly without further purification. The component complex $[Ni(Im)_6](NO_3)_2$, $[Mn(Im)_6](NO_3)_2$ and $[Cu(Me\text{-}Im)_4]Cl_2$ were prepared by the literature method [10].

#### 2.2.1. Synthesis of $[Hg(SCN)_4Ni(Im)_3]_\infty$ (1)

Compound **1** was synthesized as deep green prisms in about 85% yield by a hydrothermal method. A mixture of $NH_4SCN$ (3.0 g, 40 mmol), $Hg(NO_3)_2 \cdot H_2O$ (3.4 g, 10 mmol), $[Ni(Im)_6](NO_3)_2 \cdot 4H_2O$ (6.6 g, 10 mmol) and water (40 ml), and sealed in a 50 ml Teflon-lined reactor, which was heated to 120 °C for 3 days. After cooling to room temperature, deep green prism crystals were isolated. They were all collected, dried and submitted for elemental analysis. Anal. Calc. for $C_{13}H_{12}HgN_{10}NiS_4$ **1**: C, 22.44%; H, 1.74%; N, 20.13%; S, 18.43%. Found: C, 22.09%; H, 1.97%; N, 19.94%; S, 18.58%.

#### 2.2.2. Synthesis of $[Hg(SCN)_4Mn(Im)_2]_\infty$ (2)

A mixture of $NH_4SCN$ (3.0 g, 40 mmol), $Hg(NO_3)_2 \cdot H_2O$ (3.4 g, 10 mmol), $[Mn(Im)_6](NO_3)_2$( 5.9 g, 10 mmol) and water (40 ml), and sealed in a 50 ml Teflon-lined reactor, which was heated to 120 °C for 3 days. After cooling to room temperature, purple prism crystals were isolated. Yield 80%. Anal. Calc. for $C_{10}H_8HgMnN_8S_4$ **2**: C, 19.23%; H, 1.28%; N, 17.95%; S, 20.51%. Found: C, 19.09%; H, 1.17%; N, 17.94%; S, 19.87%.

#### 2.2.3. Synthesis of $[Hg(SCN)_4Cu(Me\text{-}Im)_3]_n$ (3)

This assembly was prepared as blue crystals in a way similar to that of compound **1**, except for the use of $[Cu(Me\text{-}Im)_4]Cl_2$ instead of $[Ni(Im)_6](NO_3)_2$. Anal. Calc. for $C_{16}H_{18}CuHgN_{10}S_4$ **3**: C, 25.87%; H, 2.44%; N, 18.86%; S, 17.27%. Found: C, 25.49%; H, 2.37%; N, 18.57%; S, 17.58%.

### 2.3. Structure determination

The summary of the key crystallographic information of compounds **1**, **2** and **3** are given in Table 1. The selected crystal was mounted on Enraf-Nonius CAD4/Mach3 diffractometer. Reflection data were measured at 20 °C using graphite monochromated $M_0$-$K_\alpha$ ($\lambda = 0.71073$ Å) radiation. The collected data were reduced by using the program SAINT [11]. The structure was solved by direct methods and refined by full-matrix least-squares method on $F^2_{obs}$ by using the SHELXTL software package [12]. All non-H atoms were anisotropically refined. The hydrogen atom positions were fixed geometrically at calculated distances and allowed to ride on the parent carbon atoms.

## 3. Results and discussion

### 3.1. Synthesis

Hydrothermal methods are important in the synthesis of novel multidimensional open-framework materials. It is known that the architectures of the products depend on many factors, such as temperature, the anions involved, the molar ratios of the precursors, the pH, etc., and subtle adjustments of these parameters often result in the formation of quite different structures [13,14]. Our syntheses under hydrothermal methods with different metal compounds in nearly same conditions provide three novel coordination polymers with different structural frameworks. The reason for the different results obtained from these reactions is perhaps due to self assemble, although the details are not clear. The thermal analysis results of complexes **1** and **3** was shown that no structural transitions were found in these two compounds before

Table 1
Summary of crystallographic data of the three compounds

| Empirical formula | $C_{13}H_{12}HgN_{10}NiS_4$ (**1**) | $C_{10}H_8HgMnN_8S_4$ (**2**) | $C_{16}H_{18}HgN_{10}CuS_4$ (**3**) |
|---|---|---|---|
| Formula weight | 695.87 | 624.01 | 742.76 |
| Temperature (K) | 293(2) | 293(2) | 293(2) |
| Wavelength (Å) | 0.71073 | 0.71073 | 0.71073 |
| Crystal system, space group | Monoclinic, $P2_1/c$ | Monoclinic, $Pc$ | Triclinic, $P\bar{1}$ |
| Unit cell dimensions | $a = 8.041(2)$ Å, $\alpha = 90°$ | $a = 8.838(2)$ Å, $\alpha = 90°$ | $a = 8.453(2)$ Å, $\alpha = 83.04(3)°$ |
| | $b = 13.352(3)$ Å, $\beta = 101.14(3)°$ | $b = 7.958(2)$ Å, $\beta = 121.58(2)°$ | $b = 9.870(2)$ Å, $\beta = 79.49(3)°$ |
| | $c = 21.034(6)$ Å, $\gamma = 90°$ | $c = 16.075(5)$ Å, $\gamma = 90°$ | $c = 15.051(3)$ Å, $\gamma = 88.40(3)°$ |
| Volume (Å$^3$) | 2215.7(9) | 963.2(4) | 1225.5(4) |
| $Z$, Calculated density (mg/m$^3$) | 4, 2.086 | 2, 2.152 | 2, 2.013 |
| Absorption coefficient (mm$^{-1}$) | 8.169 | 9.059 | 7.490 |
| $F$(000) | 1328 | 586 | 714 |
| $\theta$ rang | 1.82–25.97° | 2.56–24.98° | 1.39–24.97° |
| Limiting indices | $0 \Leftarrow h \Leftarrow 9$, $-16 \Leftarrow k \Leftarrow 0$, $-25 \Leftarrow l \Leftarrow 25$ | $0 \Leftarrow h \Leftarrow 10$, $-9 \Leftarrow k \Leftarrow 0$, $-19 \Leftarrow l \Leftarrow 16$ | $-1 \Leftarrow h \Leftarrow 10$, $-11 \Leftarrow k \Leftarrow 11$, $-17 \Leftarrow l \Leftarrow 17$ |
| Reflections collected/unique | 4657/4335 [$R$(int) = 0.0439] | 1803/1803 [$R$(int) = 0.0000] | 5072/4148 [$R$(int) = 0.0919] |
| Completeness to $\theta$ | 100.0% | 99.4% | 96.5% |
| Refinement method | Full-matrix least-squareson $F^2$ | Full-matrix least-squareson $F^2$ | Full-matrix least-squareson $F^2$ |
| Data/restraints/parameters | 4335/0/262 | 1803/3/218 | 4148/0/293 |
| Goodness-of-fit on $F^2$ | 0.979 | 1.054 | 0.957 |
| Final $R$ indices [$I > 2\sigma$ ($I$)] | $R1 = 0.0443$, w$R2 = 0.0937$ | $R1 = 0.0533$, w$R2 = 0.1321$ | $R1 = 0.0884$, w$R2 = 0.2038$ |
| $R$ indices (all data) | $R1 = 0.1472$, w$R2 = 0.1286$ | $R1 = 0.0586$, w$R2 = 0.1374$ | $R1 = 0.2083$, w$R2 = 0.2602$ |
| Extinction coefficient | | 0.016(2) | 0.0061(16) |
| Largest diff. peak and hole (e/Å$^3$) | 0.809 and −1.319 | 2.788 and −2.680 | 2.544 and −3.947 |

300 °C, which implies a high thermal stability in them (See Supporting Information S5 and S6).

### 3.2. Description of the structures

The selected bond lengths and angles with their estimated standard deviations for compounds **1**, **2** and **3** are listed in Table 2, and the molecular structures of the asymmetric units for the three compounds are shown in Fig. 1.

For complex **1**, the structure consists of a neutral chain, which is formed by an alternating $[Hg(SCN)_4]^{2-}$ and $[Ni(Im)_3]^{2+}$ units. Three thiocyanate ligands $SCN^-$ of $[Hg(SCN)_4]^{2-}$ are linked to the $[Ni(Im)_3]^{2+}$ units with the SCN–Ni. The Ni(II) ion is six-coordinated by three thiocyanate nitrogen atoms and three imidazole molecules with the slightly distorted octahedral geometry. The Hg(II) atom is coordinated with four S atoms of SCN group and has a tetrahedral geometry. Each Hg(II) ion connects to three nickel ions through three thiocyanate bridges, and one thiocyanate group is nonbridging group. For complex **2**, the structure also consists of a neutral chain, the Mn(II) ion is six-coordinated by four thiocyanate nitrogen atoms and two imidazole molecules. Four $SCN^-$ of $[Hg(SCN)_4]^{2-}$ are linked to the $[Mn(Im)_2]^{2+}$ units, each Hg(II) ion connects to four manganese ions through four thiocyanate bridges. For complex **3**, the asymmetric unit consists of two $[Hg(SCN)_4]^{2-}$ anions, one $[Cu(Me\text{-}Im)_2]^{2+}$ cation and one $[Cu(Me\text{-}Im)_4]^{2+}$ cation. Each $[Hg(SCN)_4]^{2-}$ anion coordinates with two $[Cu(Me\text{-}Im)_2]^{2+}$ (as Cu1) cations and one $[Cu(Me–Im)_4]^{2+}$ cation (as Cu2). The metal ion of Cu1 assumes an elongated octahedral coordination geometry, and each Cu1 connects to four mercury ions through four thiocyanate bridges, in which the equatorial sites are occupied by two nitrogen atoms of the methyl-imidazole ligands and two nitrogen atoms of SCN ligands, while the axial positions are occupied by two nitrogen atoms from SCN groups. The Cu2 coordination sphere can be also described as an elongated octahedral geometry with the equatorial coordinated atoms N7, N9, N7A, N9A of four methyl-imidazole groups and the axial atom N2 of SCN group. Each Cu2 ion links two mercury ions through two thiocyanate ions in the *trans* position. Thus, two kinds of copper atoms, Cu1 and Cu2, with different coordination environments exist in the crystal lattice of complex **3**. All of the Hg(II) atoms are coordinated with four SCN S atoms and have a tetrahedral geometry, with two thiocyanate bridging to Cu1 and one thiocyanate bridging to Cu2.

The Hg–S bond lengths in three complexes are normal [5,6,15], with Hg–S bond lengths in the ranges 2.494(4)–2.579(3) Å for complex **1,** 2.516(5)–2.606(6) Å for complex **2** and 2.487(7)–2.627(7) Å for complex **3**, respectively. For complex **1**, the Ni–N distances involving the nitrogen atoms from bridging thiocyanate ligands and from imidazole molecules, are respectively in the ranges 2.051(9)–2.092(9) Å and 2.101(9)–2.116(9) Å, in good agreement with those observed for the octahedrally coordinated nickel complexes [16,17]. Consequently, for each Hg atom, there are three SCN groups acting as bridging units and ones acting as terminals. Through the bridging thiocyanate groups, Hg–Ni–Hg–Ni atoms are linked to form one small 16-membered tetrametallocycle

Table 2
Selected bond lengths (Å) and angles (°)

| | | | |
|---|---|---|---|
| Compound **1** $[Hg(SCN)_4Ni(Im)_3]_n$ | | | |
| Hg(1)–S(1)$^{i}$ | 2.494(4) | Ni(1)–N(5) | 2.101(9) |
| Hg(1)–S(2)$^{ii}$ | 2.546(3) | Ni(1)–N(7) | 2.115(9) |
| Hg(1)–S(3) | 2.547(3) | Ni(1)–N(8) | 2.116(10) |
| Hg(1)–S(4) | 2.579(3) | N(3)–C(4) | 1.348(14) |
| Ni(1)–N(3) | 2.051(9) | N(4)–C(4) | 1.325(16) |
| Ni(1)–N(1) | 2.088(9) | N(4)–C(6) | 1.372(16) |
| Ni(1)–N(9) | 2.092(9) | | |
| S(1)$^{i}$–Hg(1)S(2)$^{ii}$ | 122.03(12) | N(1)–Ni(1)–N(8) | 85.0(4) |
| S(1)$^{i}$–Hg(1)–S(3) | 115.60(11) | N(9)–Ni(1)–N(8) | 91.4(4) |
| S(2)$^{ii}$–Hg(1)–S(3) | 101.31(10) | N(5)–Ni(1)–N(8) | 90.3(4) |
| S(1)$^{i}$–Hg(1)–S(4) | 106.61(14) | N(1)–Ni(1)–N(5) | 175.3(4) |
| S(2)$^{ii}$–Hg(1)–S(4) | 103.53(13) | N(9)–Ni(1)–N(5) | 90.3(4) |
| S(3)–Hg(1)–S(4) | 106.28(12) | N(3)–Ni(1)–N(7) | 92.4(4) |
| N(3)–Ni(1)–N(1) | 92.2(4) | N(1)–Ni(1)–N(7) | 90.3(4) |
| N(3)–Ni(1)–N(9) | 91.0(4) | N(9)–Ni(1)–N(7) | 176.5(4) |
| N(1)–Ni(1)–N(9) | 90.6(4) | N(5)–Ni(1)–N(7) | 88.6(4) |
| N(3)–Ni(1)–N(5) | 92.3(4) | N(7)–Ni(1)–N(8) | 85.4(4) |
| Compound **2** $[Hg(SCN)_4Mn(Im)_2]_n$ | | | |
| Hg(1)–S(2)$^{\#1}$ | 2.516(5) | Mn(1)–N(5) | 2.263(18) |
| Hg(1)–S(1)$^{\#2}$ | 2.529(5) | Mn(1)–N(8) | 2.262(17) |
| Hg(1)–S(3)$^{\#3}$ | 2.606(6) | Mn(1)–N(7) | 2.239(19) |
| Hg(1)–S(4) | 2.536(6) | Mn(1)–N(6) | 2.237(17) |
| Mn(1)–N(1) | 2.194(16) | Mn(1)–N(3) | 2.235(16) |
| S(2)$^{\#1}$–Hg(1)–S(1)$^{\#2}$ | 109.45(18) | S(2)$^{\#1}$–Hg(1)–S(4) | 105.1(2) |
| S(1)$^{\#2}$–Hg(1)–S(4) | 118.3(3) | N(1)–Mn(1)–N(6) | 176.4(7) |
| S(2)$^{\#1}$–Hg(1)–S(3)$^{\#3}$ | 106.32(19) | N(3)–Mn(1)–N(6) | 89.6(7) |
| N(1)–Mn(1)–N(3) | 93.9(6) | N(6)–Mn(1)–N(7) | 86.6(7) |
| N(1)–Mn(1)–N(7) | 89.9(7) | N(1)–Mn(1)–N(8) | 89.7(7) |
| N(3)–Mn(1)–N(8) | 88.8(8) | N(6)–Mn(1)–N(8) | 89.2(7) |
| Compound **3** $[Hg(SCN)_4Cu(Me–Im)_3]_n$ | | | |
| Hg(1)–S(1) | 2.487(7) | N(5)–C(5) | 1.30(3) |
| Hg(1)–S(2) | 2.501(7) | N(5)–C(6) | 1.37(3) |
| Hg(1)–S(3) | 2.502(6) | N(6)–C(7) | 1.34(3) |
| Hg(1)–S(4) | 2.627(7) | N(6)–C(5) | 1.38(3) |
| Cu(1)–N(5) | 1.964(18) | Cu(1)–N(4)$^{iii}$ | 2.04(2) |
| S(1)–Hg(1)–S(2) | 112.8(3) | S(1)–Hg(1)–S(3) | 106.5(2) |
| S(2)–Hg(1)–S(3) | 110.2(2) | C(1)–S(1)–Hg(1) | 99.0(12) |
| S(1)–Hg(1)–S(4) | 102.7(2) | C(2)–S(2)–Hg(1) | 101.2(8) |
| S(2)–Hg(1)–S(4) | 111.9(2) | C(3)–S(3)–Hg(1) | 96.6(7) |
| S(3)–Hg(1)–S(4) | 112.5(3) | C(4)–S(4)–Hg(1) | 106.5(7) |
| N(5)–Cu(1)–N(4)$^{iii}$ | 91.0(8) | N(7)–Cu(2)–N(9)$^{iv}$ | 89.2(8) |

[a]Symmetry relation, $^{i}$means $-x-1$, $y-1/2$, $-z+3/2$, $^{ii}$means $x$, $-y+1/2$, $z-1/2$, $^{iii}$means $x$, $y-1$, $z$, $^{iv}$means $-x+2$, $-y+1$, $-z$, $^{\#1}$means $x-1$, $-y$, $z-1/2$, $^{\#2}$means $x-1$, $y+1$, $z$, $^{\#3}$means $x$, $y+1$, $z$.

$[Hg_2(SCN)_4Ni_2]$ and one big 32-membered octametallocycle $[Hg_4(SCN)_8Ni_4]$. As a result, the small 16-membered rings share the same lateral (Hg–S–C–N–Ni) with four big 32-membered rings to form a "flower-like" motif. The small 16-membered ring is pistil, and the four big 32-membered rings are petal (See Fig. 2). By sharing the small rings, these "flower" are connected to each other to lead to two-dimensional infinite chains extended along the *b*-axis.

For complex **2**, the Mn–N distances are normal [2.19 (2)–2.26 (2) Å] for the octahedrally coordinated manganese complexes [18,19]. Four SCN groups of $[Hg(SCN)_4]^{2-}$ all act as bridging units and link Mn and Hg atom to form two small 8-membered bimetallocycle $[Hg(SCN)_2Mn]$ and one big 24-membered hexametallocycle $[Hg_3(SCN)_6Mn_3]$ (See Fig. 3 top). For complex **3**, two copper(II) atoms all assumes an elongated octahedral coordination geometry with the Cu–$N_{eq}$ bond distances in the range of 1.964(8)–2.045(8) Å for Cu1 and 1.991(8)–2.041(8) Å for Cu2, while the axial positions are all occupied by two nitrogen atoms from $SCN^-$ groups with Cu–$N_{ax}$ distances of 2.504(8) Å for Cu1 and 2.609(8) Å for Cu2, respectively. Due to the Jahn–Teller effects, the Cu–$N_{ax}$ distances are much longer than the Cu–$N_{eq}$ bond distances, but they are comparable with those observed in other similar cyanometalate analogs [20,21]. As usual, the $[Hg(SCN)_4]^{2-}$ fragment exhibits a slightly distorted tetrahedral structure.

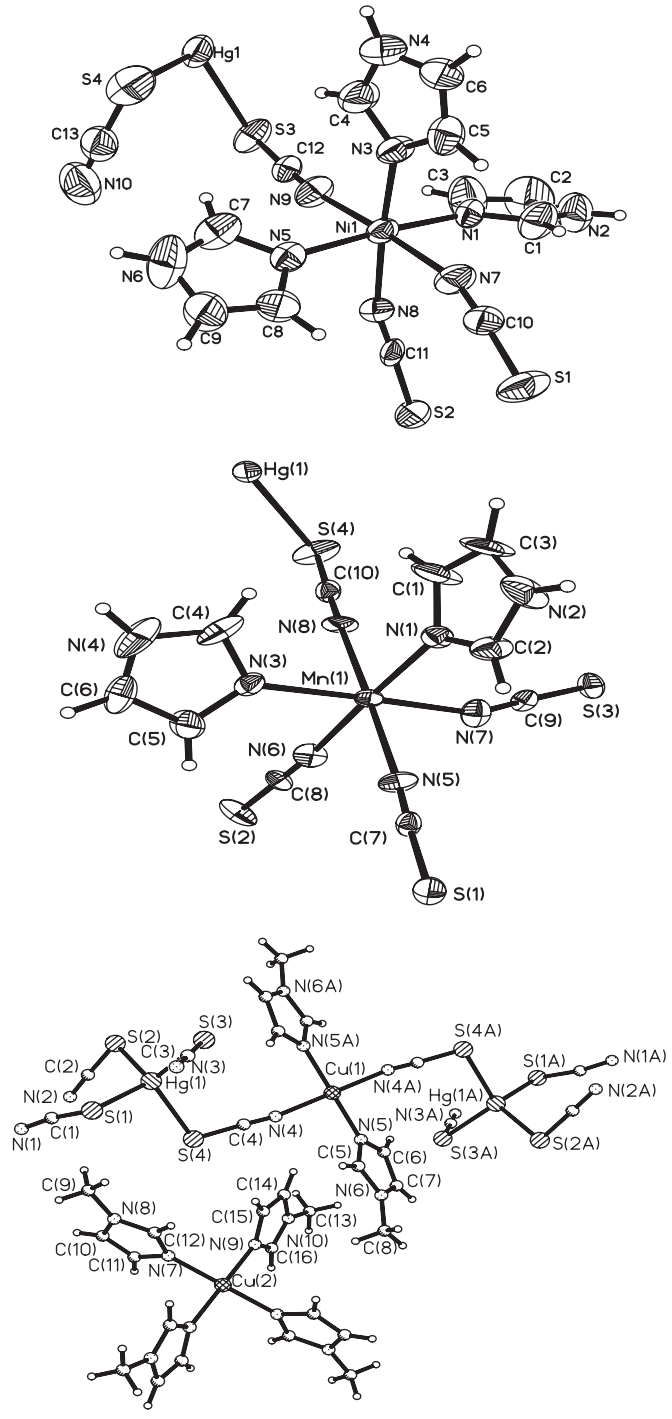


Fig. 1. Molecular structures for complexes **1** (top), **2** (middle) and **3** (bottom).

Each Hg atom, there are three SCN groups acting as bridging units and ones acting as terminals. As similar as compound **1**, through the bridging thiocyanate groups, the compound **3** also form two metallocycles: Hg–Cu1–Hg–Cu1 atoms are linked to form one small 16-membered tetrametallocycle and Hg–Cu1–Hg–Cu2 form one big 32-membered octametallocycle. Like compound **1**, the small 16-membered rings share the same lateral (Hg–S–C–N–Cu1) with four big 32-membered rings to

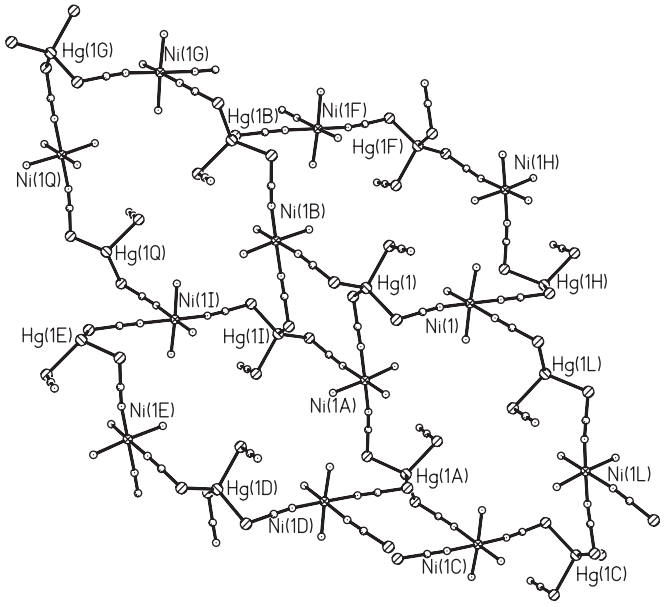


Fig. 2. A fragment of **1** along the *b*-axis, showing the "flower-like" structure. Perspective view of the two-dimensional structure of **1** onto the bc plane. The imidazole ligands are omitted for clarity.

form a "flower-like" motif. The small 16-membered ring is pistil, and the four big 32-membered rings are petal (see Fig. 3 bottom).

The intramolecular metal–metal separations in complex **1** and **2** are 5.604 and 5.930 Å for Hg···Ni and Ni···Hg, and 5.905 and 6.258 Å for Hg···Mn and Mn···Hg, respectively. The shortest intermolecular M···M distances are 8.041 Å for complex **1** and 8.838 Å for complex **2**, respectively. For complex **3,** the intramolecular Hg···Cu1 and Hg···Cu2 separations are 6.492 and 6.534 Å, respectively. The shortest intermolecular Hg···Hg, Cu1···Cu2, and Cu···Cu distances are 6.258, 7.931 and 12.814 Å, respectively.

### 3.3. Magnetic properties and ESR spectra

The magnetic properties of complex **1** have been investigated in the 1.8–300 K temperature range. The $\chi_M T$ versus $T$ plot continuously decreases or increases upon cooling down according to whether the interaction is antiferro- or ferromagnetic [22]. The $\chi_M T$ versus $T$ plots for the complex **1** is shown in Fig. 4. The $\chi_M T$ product at room temperature is about 1.82 emu K mol$^{-1}$; they decrease smoothly upon cooling, reach the minimum around 12.0 K, increase smoothly upon cooling further, and reach a maximum at ca. 7.0 K. After this maximum, the $\chi_M T$ values decreases rather rapidly and makes a sharp peak. Between 300 and 12 K, an antiferromagnetic behavior is observed. Starting from 12 K, $\chi_M T$ values increase to 1.80 emu K mol$^{-1}$ 7.0 K, indicating the presence of ferromagnetic coupling [23]. Upon further cooling below 7.0 K, the $\chi_M T$ values decrease to 1.71 emu K mol$^{-1}$ at 1.8 K. This low-temperature decrease could be due to weak

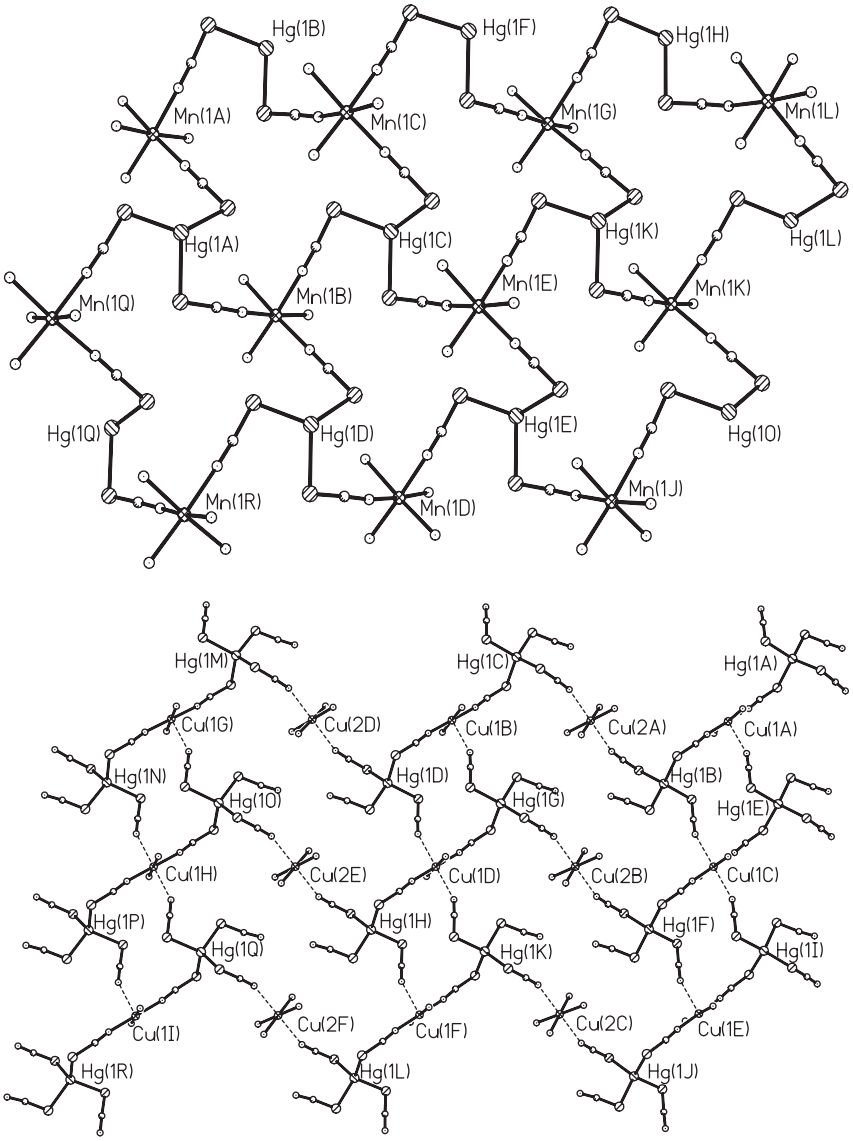


Fig. 3. A view of a fragment of 2D structure along the *bc* plane for **2** (top) and **3** (bottom). The imidazole rings of **2** and **3** have been omitted for clarity.

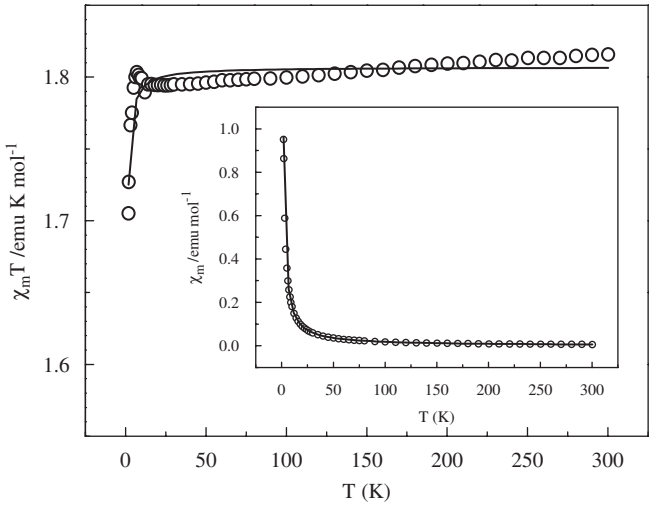


Fig. 4. Variable temperature magnetization for complex **1** in the form $\chi_M T$ vs. $T$. The solid line is the fitting result. Inset is the plot of $\chi_M T$ vs. $T$.

antiferromagnetic coupling or the zero-field splitting of the ground state [24]. This is irregular spin state structure, and this behavior has been observed in some compounds, such as, $\{Ni(Me_6\text{-}[14]\text{-}ane\text{-}N_4)_2Cu(pba)\}(ClO_4)_2$ and $\{Mn(Me_6\text{-}[14]\text{-}ane\text{-}N_4)_2Cu(pba)\}(CF_3SO_3)_2 \cdot H_2O$ [22], $[Ni(bapa)(H_2O)Cu(pba)] \cdot 2H_2O$ and $\{[Ni(bapa)(H_2O)]_2Cu(pba)\}(ClO_4)_2$ [25], $[L_2Fe_2(dmg)_3Ni]$ $(PF_6)_2 \cdot 0.5CH_3OH$ [$L$ = 1,4,7-Trimethyl-1,4,7-triazacyclononane; dmg = Dimethylglyoximate)] [26] and some oxamato-bridged trinuclear $Ni^{II}Cu^{II}Ni^{II}$ complexes, etc [27]. The antiferromagnetic interaction between neighboring local spins ($Ni^{II}Hg^{II}Ni^{II}$ for complex **1**) will align the two large local spins in a parallel fashion, that is, the small central spin polarizes the two large terminal spins in a ferromagnetic-like fashion [27,28].

To fit the experimental values, we have made several approaches. We only consider the high-temperature region, cutting the experimental curve at different temperatures and fitting with the typical formula given in the literature

[29] for a linear multinuclear $Ni^{II}$ complex, using the Hamiltonian $H = -J\Sigma S_i S_j$, and obtaining the susceptibility per $g$-atom of Ni, the result is

$$\chi_{Ni} = \frac{Ng^2\beta^2}{3kT} S_{Ni}(S_{Ni}+1)\chi_M = \frac{\chi_{Ni}}{1-(2zj'/Ng^2\beta^2)\chi_{Ni}},$$

$zJ$ represents the magnetic interaction between adjacent nickel(II) metal ions. $J$ is negative or positive according to whether the interaction is antiferro- or ferromagnetic. The best fit is obtained by cutting at 15 K with the following parameters: $z = 20$, $g = 2.6884$, $zJ = -0.0443\,cm^{-1}$, $R = 18.6 \times 10^{-5}$.

The powder ESR spectra were recorded on a Bruker 2000-SRC spectromter. The room temperature ESR spectra of the complexes **1** and **3** are shown in Fig. 5. Because $Hg^{2+}$ is $d^{10}$ a diamagnetic atom, it show that $[Hg(SCN)_4]^{2-}$ exhibits no ESR signals by itself. The dominant signal must arise from multinuclear $Ni^{2+}$ and $Cu^{2+}$ center, or the interaction between $Hg^{2+}$ and $Ni^{2+}$ or $Cu^{2+}$. The six-coordinate Ni(II) complexes have an unpaired electron in the $d_{x^2-y^2}$ orbital, as well as one in the $d_{z^2}$ orbital. Therefore, in the case of complex **1** one can expect magnetic interactions between the $Ni^{2+}$ ions and $Ni^{2+}$ ions, as well as between the $Ni^{2+}$ ions and coordination nitrogen atoms. As can be seen from Fig. 5 (top), the spectrum of complex **1** shows the strong anisotropy of the $g$-factor as well as the hyperfine coupling constant corresponding to the signals of six-coordinate Ni(II) ions [30,31]. The complex **1** displays two resonance bands: one centered at $g = 2.2377$ and the other at about $g = 4.0878$. The spin couplings in $Ni^{II}Hg^{II}Ni^{II}$ species give rise to two $S = 1/2$ and two $3/2$ states. Both $S = 1/2$ and $S = 3/2$ spin states can originate through exchange coupling. The $g$ values correspond to a Kramers doublet which must be the ground state of the pair. This might in principle correspond to a $S = 1/2$ spin state or to a $S = 3/2$ largely split in zero magnetic field. However in the latter case at least one $g$ value should be larger than 4, if the true $g$ values of the pair are close to 2 [32]. Due to zero-field splitting (ZFS) effects, the allowed transitions within the

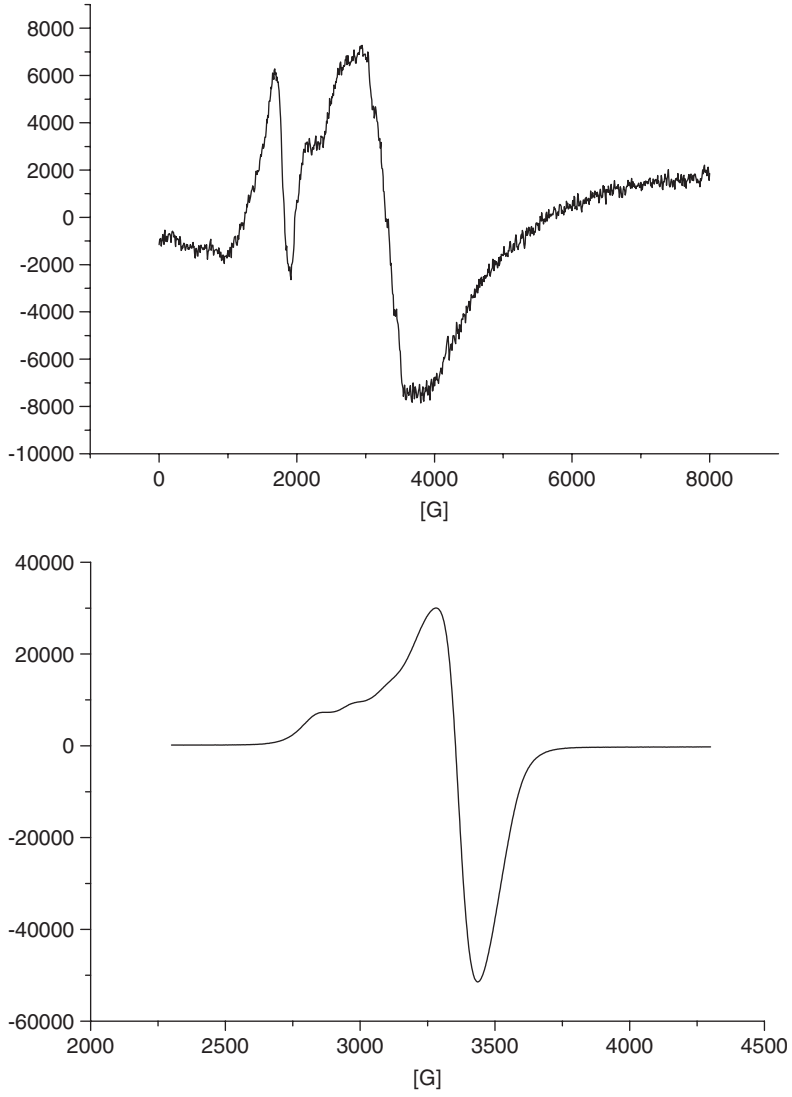


Fig. 5. Polycrystalline X-band ESR spectra of complexes **1** (top) and **3** (bottom) at room temperature.

quarter or sextuplet states will produce two resonant signals: one at the high field near $g = 2$ and the other at a low field with $g > 4$, assuming that the zero-field splitting is axial [33]. The spectrum of complex **3** (Fig. 5 bottom), exhibiting two types of $g$ values, $g_{\|}$ and $g_{\perp}$, have been used to distinguish unambiguously between $d_{x^2-y^2}$ and $d_{z^2}$ ground states for which $g_{\|} > g_{\perp}$ and $g_{\perp} > g_{\|} \approx 2.00$, respectively [34]. The complex **3** studied here shows a pronounced peak ($g_{\perp} = 2.1783$) and another pronounced peak ($g_{\|} = 2.5658$) typical of a $d^9$ complex possessing axial symmetry, which suggested that the ground state was $d_{x^2-y^2}$ orbital with the unpaired electron and the coordination geometry was octahedral or square-pyramidal [33,35]. These results are consistent with the crystal structure in demonstrating $Cu^{2+}$ ion of octahedral environment. In axial symmetry the $g$ values are related by the expression $G = (g_{\|}-2)/(g_{\perp}-2)$, which measures the exchange interaction between copper centers in the polycrystalline solid. If $G > 4$, the exchange interaction is negligible; $G < 4$ indicates considerable exchange interaction. In this complex, $G = 3.17$ indicates there is a weak interaction between Cu atoms.

## 4. Conclusions

Three novel heterobimetallic thiocyanato-bridged coordination polymers have been obtained by hydrothermal synthesis. All coordination polymers possess 3-D structures, and consist of organic base neutral ligands (imidazole and *N*-methyl-imidazole) and $SCN^{-1}$ anions. Their structural difference is mainly caused by the role of the organic base and metal ions. In three complexes, SCN groups exist as bridge to coordinate simultaneously with Hg and *M* (*M* = Ni, Mn, Cu) and to form interpenetration networks. The successful isolations of the three compounds demonstrate that it is promising to apply organic base neutral ligands and $[Hg(SCN)_4]^{2-}$ salts in the designed syntheses of novel coordination polymers under hydrothermal reacting conditions. The $\chi_M T$ versus $T$ plots for complex **1** exhibit the minimum characteristic of antiferromagnetically coupled NiHgNi species with an irregular spin state structure. The ESR measurement of complex **1** shows that the $Ni^{II}$ in octahedral surrounding has two unpaired electrons in $e_g$ orbital. From the ESR spectra of complex **3**, we can conclude that the $Cu^{II}$ atom is in six-coordinated crystal field environment.

## 5. Supplementary material

Crystallographic data for the structural analyses have been deposited with the Cambridge Crystallographic Data Centre, CCDC-285475 for complex **1,** CCDC-290146 for complex **2** and CCDC-285474 for complex **3** contain the supplementary crystallographic data for this paper. These data can be obtained free of charge from the *Cambridge Crystallographic Data Centre* via www.ccdc.cam.ac.uk/data_request/cif.

## Acknowledgments

This work was supported by Natural Science Foundation of Shandong Province (No.Y2005B04), China.

## References

[1] (a) D.E. Vos, F.T. Starzyk, P.A. Jacobs, Angew. Chem. Int. Ed. Engl. 33 (1994) 431;
(b) A.L. Balch, M. Mazzanti, T.M. St. Claire, M.M. Olmstead, Inorg. Chem. 34 (1995) 2194;
(c) A.L. Balch, M. Mazzanti, T.M. St. Claire, J. Chem. Soc., Chem. Commun. (1994) 269.
[2] (a) N.L. Rosi, J. Eckert, M. Eddaoudi, D.T. Vodak, J. Kim, M. O'Keeffe, O.M. Yaghi, Science 300 (2003) 1127;
(b) O.M. Yaghi, M. O'Keeffe, N.W. Ockwig, H.K. Chae, M. Eddaoudi, J. Kim, Nature 423 (2003) 705;
(c) N.L. Rosi, M. Eddaoudi, J. Kim, M. O'Keeffe, O.M. Yaghi, Angew. Chem. Int. Ed. 41 (2002) 284.
[3] (a) S.W. Zhang, D.G. Fu, W.Y. Sun, Z. Hu, K.B. Yu, W.X. Tang, Inorg. Chem. 39 (2000) 1142;
(b) D.F. Li, S. Gao, L.M. Zheng, W.X. Tang, J. Chem. Soc. Dalton Trans. (2002) 2805.
[4] (a) J.C. Liu, G.C. Guo, J.S. Huang, X.Z. You, Inorg. Chem. 42 (2003) 235;
(b) H. Zhao, Z.R. Qu, Q. Ye, X.S. Wang, J. Zhang, R.G. Xiong, X.Z. You, Inorg. Chem. 43 (2004) 1813.
[5] Y. Sungho, J.L. Stephen, J. Am. Chem. Soc. 126 (2004) 2666.
[6] (a) X.Q. Wang, W.T. Yu, D. Xu, M.K. Lu, D.R. Yuan, J.R. Liu, G.T. Lu, Acta Crystollogr C 56 (2000) 1305;
(b) X.Q. Wang, W.T. Yu, D. Xu, M.K. Lu, D.R. Yuan, G.T. Lu, Acta Crystollogr C 58 (2002) m341.
[7] (a) M.B. Cingi, A.M.M. Lanfredi, A. Tiripicchio, J.G. Haasnoot, J. Reedijk, Inorg. Chim. Acta 101 (1985) 49;
(b) M.R. Udupa, B. Krebs, Inorg. Chim. Acta 42 (1980) 37.
[8] P. Brooks, N. Davidson, J. Am. Chem. Soc. 82 (1960) 2118.
[9] (a) F.F. Jian, P.S. Zhao, H.L. Xiao, S.S. Zhang, Chin. J. Chem. 20 (2002) 1134;
(b) F.F. Jian, Z.X. Wang, Z.P. Bai, X.Z. You, W. Chen, Trans. Met. Chem. 24 (1999) 589;
(c) F.F. Jian, Q.X. Wang, P.P. Sun, J. Kui, Chin. J. Inorg. Chem. 20 (5) (2004) 581.
[10] F.F. Jian, Y.P. Tong, H.L. Xiao, Q.X. Wang, K. Jiao, Chin. J. Struct. Chem. 23 (9) (2004) 979.
[11] G.M. Sheldrick, SAINT v4 Software Reference Manual, Siemens Analytical X-ray Systems, Inc., Madison, Wisconsin, USA, 1996.
[12] G.M. Sheldrick, SHELXTL, v5 Reference Manual, Siemens Analytical X-ray *Sysytems*, Inc., Madison, Wisconsin, USA, 1996.
[13] P.M. Forster, A.R. Burbank, C. Livage, G. Ferey, A.K. Cheetham, Chem. Commun. (2004) 368.
[14] X. He, C.Z. Lu, D.Q. Yuan, S.M. Chen, J.T. Chen, Eur. J. Inorg. Chem. (2005) 2181.
[15] (a) X.Q. Wang, W.T. Yu, D. Xu, M.K. Lu, D.R. Yuan, G.T. Lu, Acta Crystollogr C56 (2000) 647;
(b) X.Q. Wang, W.T. Yu, D. Xu, M.K. Lu, D.R. Yuan, Acta Crystollogr C56 (2000) 418.
[16] D. Guo, C.Y. Duan, C.J. Fang, Q.J. Meng, J. Chem. Soc. Dalton Trans. 00 (2002) 834.
[17] M.K. Saha, M.C. Moron, F. Palacio, I. Bernal, Inorg. Chem. 44 (2005) 1354.
[18] L. Toma, R. Lescouezec, J. Vaissermann, F.S. Delgado, C. Ruiz-Perez, R. Carrasco, J. Cano, F. Lloret, M. Julve, Chem. Eur. J. 10 (2004) 6130.
[19] U. Ray, S. Jasimuddin, B.K. Ghosh, M. Monfort, J. Ribas, G. Mostafa, T. -H. Lu, C. Sinha, Eur. J. Inorg. Chem. (2004) 250.
[20] D.F. Li, S. Gao, L.M. Zheng, W.Y. Sun, T. Okamura, N. Ueyama, W.X. Tang, New J. Chem. 26 (2002) 485.

[21] X.P. Shen, S. Gao, G. Yin, K.B. Yu, Z. Xu, New J. Chem. 28 (2004) 996.
[22] Y. Pei, Y. Journaux, O. Kahn, Inorg. Chem. 27 (1988) 399.
[23] F.C. Liu, Y.F. Zeng, J.R. Li, X.H. Bu, H.J. Zhang, J. Ribas, Inorg. Chem. 44 (2005) 7298.
[24] C.D. Wu, C.Z. Lu, W.B. Yang, H.H. Zhuang, J.S. Huang, Inorg. Chem. 41 (2002) 3302.
[25] J. Ribas, C. Diaz, R. Costa, Y. Journaux, C. Mathoniere, O. Kahn, A. Gleizes, Inorg. Chem. 29 (1990) 2042.
[26] P. Chaudhuri, M. Winter, B.P.C. Della Vedova, P. Fleischhauer, W. Haase, U. Florke, H.J. Haupt, Inorg. Chem. 30 (1991) 4777.
[27] E.Q. Gao, J.K. Tang, D.Z. Liao, Z.H. Jiang, S.P. Yan, G.L. Wang, Inorg. Chem. 40 (2001) 3134.
[28] O. Kahn, Adv. Inorg. Chem. 43 (1996) 179.
[29] A.P. Ginsberg, R.L. Martin, R.C. Sherwood, Inorg. Chem. 7 (1968) 932.
[30] A.R. Harutyunyan, A.A. Kuznetsov, Chem. Phys. Lett. 241 (1995) 168.
[31] M. Yamashita, Y. Nonaka, S. Kida, Y. Hamaue, R. Aoki, Inorg. Chim. Acta 52 (1981) 43.
[32] L. Banci, A. Bencini, C. Benelli, A. Dei, D. Gatteschi, Inorg. Chem. 20 (1980) 1399.
[33] (a) A. Escuer, R. Vicente, J. Ribas, R. Costa, X. Solans, Inorg. Chem. 31 (1992) 2627;
(b) R. Vicente, A. Escuer, J. Ribas, Polyhedron 11 (1992) 857.
[34] B.J. Hathaway, A.A.G. Tomlinson, Coord. Chem. Rev. 5 (1970) 1.
[35] C. Jubert, A. Mohamadou, C. Gerard, S. Brandes, A. Tabard, J.P. Barbier, Inorg. Chem. Commun. 6 (2003) 900.